ELSEVIER

Journal of Fluids and Structures 21 (2005) 25–40

JOURNAL OF FLUIDS AND STRUCTURES

www.elsevier.com/locate/jfs

Blind predictions of laboratory measurements of vortex-induced vibrations of a tension riser

J.R. Chaplin[a,*], P.W. Bearman[b], Y. Cheng[c], E. Fontaine[d], J.M.R. Graham[b], K. Herfjord[e], F.J. Huera Huarte[b], M. Isherwood[f], K. Lambrakos[c], C.M. Larsen[g], J.R. Meneghini[h], G. Moe[i], R.J. Pattenden[a], M.S. Triantafyllou[j], R.H.J. Willden[b]

[a]*School of Civil Engineering and the Environment, University of Southampton, UK*
[b]*Department of Aeronautics, Imperial College of Science, Technology and Medicine, London, UK*
[c]*Technip, Houston, USA*
[d]*Institut Français du Pétrole, Rueil Malmaison, France*
[e]*Norsk Hydro, Oil and Energy, Bergen, Norway*
[f]*Orcina Ltd, Ulverston, UK*
[g]*Department of Marine Technology, Norwegian University of Science and Technology, Trondheim, Norway*
[h]*Department of Mechanical Engineering, Escola Politécnica da Universidade de São Paulo, Brazil*
[i]*Department of Civil and Transport Engineering, Norwegian University of Science and Technology, Trondheim, Norway*
[j]*Department of Ocean Engineering, Massachusetts Institute of Technology, Cambridge, MA, USA*

Received 15 December 2004; accepted 28 May 2005

Abstract

This paper compares laboratory measurements of the vortex-induced vibrations of a riser in a stepped current with blind predictions obtained with 11 different numerical models. Results are included on in-line and transverse displacements and curvatures, and dominant frequencies. In general, empirical models were more successful at predicting cross-flow displacements and curvatures than current codes based on CFD. Overall ratios between predictions and measurements of cross-flow displacements were around 95% and 75%, respectively. Predictions of cross-flow curvatures were more scattered, and almost all were unconservative. In-line vortex-induced curvatures, which may cause as much damage as cross-flow curvatures, could not be computed by any of the empirically based codes, and in general those based on CFD were in very poor agreement with the measurements.

Keywords: Vortex-induced vibrations; Riser; CFD; Numerical modelling; Blind predictions; Multi-mode response

1. Introduction

Good quality measurements of the multi-mode response of a long tension riser to vortex excitation in a nonuniform flow are in short supply. This is a handicap for those who are developing numerical models for the prediction of vortex-induced displacements and fatigue damage in risers because all computational approaches to this problem rely (and for

*Corresponding author. Tel.: +44 23 8059 2843; fax: +44 23 8067 7519.
E-mail address: j.r.chaplin@soton.ac.uk (J.R. Chaplin).

0889-9746/$ - see front matter © 2005 Elsevier Ltd. All rights reserved.
doi:10.1016/j.jfluidstructs.2005.05.016

the foreseeable future will continue to rely) on simplifying assumptions that need empirical validation. Field measurements can provide some overall indications of the accuracy of predicted displacements, curvatures and frequencies, but in general they are characterized, understandably, by inadequate documentation of the ambient conditions (to which structural responses may be very sensitive), and by sparse instrumentation and instrument failures. To be suitable for code validation, measurements must be sufficiently resolved in time and space to capture detailed features of the response, as well as a comprehensive description of the boundary conditions, such as the profile of the incident flow. At the present stage of code development, this is more important than achieving a realistic current profile or riser geometry.

Following the completion of laboratory measurements of the vortex-induced vibrations of a model riser in a stepped current in May 2003, 10 groups of code developers and users carried out blind predictions of displacements, curvatures and frequencies on up to 15 test cases with 11 different numerical models. The first exposure of some of the results was at the International Conference on Flow Induced Vibration in July 2004 (Chaplin et al., 2004). The present paper provides a more comprehensive analysis of these data, and incorporates the results of subsequent improvements in the techniques used to process the original measurements.

2. Test conditions

In the experiments that form the focus of this exercise, measurements were made of the in-line and cross-flow motion of a vertical model riser in a stepped current. The riser was 13.12 m long and 28 mm diameter, and was tested in conditions in which its lower 45% was in a uniform current of speeds up to 1 m/s, while the upper part was in still water. The in-line and transverse displacements of the riser were inferred from measurements of bending strain on its central core at 32 equally spaced points over its length.

The experiments were carried out at the Delta Flume of Delft Hydraulics, using a purpose-built structure mounted on the flume carriage. The layout is shown in Fig. 1. The riser passed through the depth of water in the flume and up to the top of a tank (the 'vacuum tank') which was open at the bottom at an elevation just below the surrounding water surface in the flume. The vacuum tank was otherwise sealed and, during the experiments to which this paper refers, it was almost filled with water by evacuating air from the top. When the carriage was moving, the riser thus experienced a stepped current consisting of uniform flow over its lower part and still water elsewhere, as shown in Fig. 1. Further details of the experiments are given by Chaplin et al. (2005).

The model riser consisted of a phosphor-bronze spine inside a fluoroplastic tube of wall thickness 0.5 mm and outer diameter 28 mm. Strain gauges were installed on flats machined into the 8 mm circular core at intervals of 410 mm over its entire length to measure its curvature about two axes. The riser was installed with universal joints at each end, and at

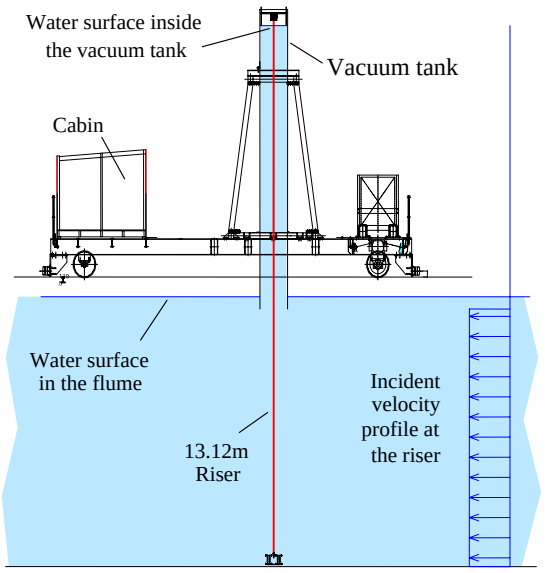

Fig. 1. Layout of the experiments. The supporting structure for the bottom of the riser is not shown.

Table 1
Test conditions for blind predictions

Case	Speed (m/s)	Top tension (N)
1	0.16	405
2	0.21	407
3	0.31	457
4	0.40	506
5	0.54	598
6	0.60	670
7	0.70	743
8	0.85	923
9	0.95	1002
10	0.11	803
11	0.41	840
12	0.51	872
13	0.21	1916
14	0.40	1926
15	0.71	2018

The top tensions are those measured during the tests.

Table 2
Definition of key parameters

Parameter	Definition
Time-averaged in-line displacement	$\bar{x}(z) = \text{mean}\,[x(z,t)]$
Envelopes of in-line displacement	$x_{\min}(z) = \min\,[x(z,t)]$, $x_{\max}(z) = \max\,[x(z,t)]$
Envelopes of cross-flow displacement	$y_{\min}(z) = \min\,[y(z,t)]$, $y_{\max}(z) = \max\,[y(z,t)]$
Maximum time-averaged in-line displacement	$\bar{x}_{\max} = \max\,[\bar{x}(z)]$
Maximum in-line displacement from the mean	$(x-\bar{x})_{\max} = \max\lvert x(z,t) - \bar{x}(z)\rvert$
Maximum cross-flow displacement	$y_{\max} = \max\,[-y_{\min}(z)\,,\ y_{\max}(z)]$
Standard deviations of curvature over time	$\sigma_{c,x}(z) = \text{st. dev.}[c_x(z,t)]$, $\sigma_{c,y}(z) = \text{st. dev.}[c_y(z,t)]$
Maximum standard deviation of curvature	$c_{x,\,\max} = \max\,[\sigma_{c,x}(z)]$, $c_{y,\,\max} = \max\,[\sigma_{c,y}(z)]$
Root-mean-square values of the standard deviation of curvature	$c_{x,\,\text{rms}} = \text{r.m.s}\,[\sigma_{c,x}(z)]$, $c_{y,\,\text{rms}} = \text{r.m.s}\,[\sigma_{c,y}(z)]$

the top it was suspended from an array of extension springs whose pre-tension could be adjusted from outside the vacuum tank.

Blind predictions of the riser's response were carried out for the conditions set out in Table 1. Measured and computed data presented below refer to in-line and transverse displacements $x(z,t)$ and $y(z,t)$, respectively, where z is measured vertically from the bottom of the riser, and t is time. The corresponding curvatures are denoted by $c_x(z,t)$ and $c_y(z,t)$. Some specific parameters are defined in Table 2. Comparisons are also made between measured and computed cross-flow frequencies f_y and mode numbers n_y. Frequencies are expressed in the form of a Strouhal number $S = f_y d/U$, where U is the incident flow speed over the lower part of the riser, and d its diameter.

3. Numerical models

The eleven numerical models used in this exercise fall into three groups. First, in four codes (identified as Norsk Hydro, USP, DeepFlow, and VIVIC) Computational Fluid Dynamics techniques are used to compute two-dimensional flow around the riser on a large number of horizontal planes distributed over its length. In this strip theory approach the only communication between the flows on different planes is through the motion of the riser, whose position was

generally updated at each time step in response to the computed instantaneous flow-induced force at each level. Secondly, two codes (Orcina Vortex Tracking and Orcina Wake Oscillator) use the same strip theory approach, but adopt more pragmatic methods to compute the force on the riser on each plane. The codes in these two groups all operate in the time domain.

The third group (VIVA, VIVANA, VICoMo, SHEAR7 and ABAVIV) variously uses data from measurements on rigid cylinders undergoing vortex-induced or forced vibrations to identify the amplitude of the mode (or range of modes) most likely to be excited. In most of these models no attempt is made to compute the in-line response. There follows a brief description of each code.

3.1. Norsk hydro

These computations use two basic programs, *Navsim* (Herfjord, 1996) for the CFD calculations on each plane and *Usfos* (Eberg et al., 1993), a structural code that accommodates nonlinear deformations and material properties. The communication between these two modules is organized by a coupler module (Herfjord et al., 1998). The whole suite is described by Herfjord et al. (1999).

Navsim uses a finite element method on a grid of triangular elements in which the flow variables are represented with linear interpolation functions. As far as possible, the CFD computations for each plane are handled by one CPU. Using results from each plane, the coupler assembles the load vector for the whole riser and passes it to *Usfos* for the structural analysis. In the next phase, the coupler receives the computed response and distributes this information to each plane, allowing the CFD computations to proceed. This interaction takes place at each time step throughout the simulation.

3.2. USP (University of São Paulo)

The USP code uses discrete vortices with a stream-function-based boundary integral approach and incorporates the growing core size or core spread method in order to model the diffusion of vorticity. The circumference of the riser is discretized into a number of panels, and from each one at each time step a discrete vortex is created at a certain offset from the boundary. Each vortex is convected with a velocity which is the sum of the free-stream velocity and that induced by all other vortices. Forces on the body are calculated by integrating viscous stresses (obtained from velocities in the near-wall region) and pressures (calculated by relating the vorticity flux on the wall to the generation of circulation). Further details can be found in Yamamoto et al. (2004).

The dynamic response of the riser is computed in the time domain with a finite element structural model based on the Euler–Bernoulli beam theory (Patel and Witz, 1991; Ferrari, 1998). A mass lumped matrix is constructed and the damping matrix is evaluated in a global manner. A stiffness matrix is obtained from an initial static analysis of the riser, displaced by steady drag loading.

3.3. Deepflow (Institut Francais du Pétrole)

On each CFD plane the two-dimensional Reynolds-averaged Navier-Stokes equations are solved using a vorticity/stream function formulation (Etienne, 1999) over an Eulerian domain surrounding the riser. The Poisson equation for the stream function is solved with a spectral method in the azimuthal direction and a fourth-order Hermitian finite difference scheme in the radial direction. The vorticity transport equation is discretized using a finite volume technique. Convective terms are treated using QUICK and TVD schemes, while the diffusive term is evaluated using second-order centered differences. An ADI algorithm is used for the temporal integration.

This Eulerian computation may be coupled with a purely Lagrangian method to describe the long time evolution of the wake. For the present problem, the CFD code was coupled with the FEM software DeepLines (2002) for the analysis of the dynamic response of risers, mooring lines and flowlines.

3.4. VIVIC (Imperial College, London)

The velocity-vorticity formulation of the Navier-Stokes equations is solved on each plane using a hybrid Eulerian–Lagrangian Vortex-in-Cell method. A time split approach is followed, whereby the diffusion of vorticity is treated in an Eulerian fashion by modelling the flow variables using linear finite elements on an unstructured triangular mesh, and the convection of vorticity is handled using a Lagrangian approach that employs discrete point vortices. At high Reynolds numbers the effects of turbulent length scales are modelled using Large Eddy Simulation with a simple volume average box filter to separate the resolvable and sub-grid flow scales.

Each time step commences with the computation of the evolution of the flow in each of the CFD planes. The computed fluid forces are then mapped to a fully (geometrically) nonlinear structural dynamics model of the riser, and the resulting displacements are advanced in time and then passed back to the CFD planes in order to start the next time step. The code is fully parallelized and the flow evolution in each CFD plane is computed on a separate processor. Details of VIVIC are given in Willden (2003) and Willden and Graham (2004).

3.5. *Orcina vortex tracking model*

This uses a two-dimensional vortex tracking model based on work by Sarpkaya and Shoaff (1979). It has two principal elements: a boundary layer model for determining the angular position of the two separation points (and the rate of generation of vorticity at each one), and a fluid convection model for computing the subsequent movement of the vortices, and the flow-induced forces. This approach has the advantage that it is computationally much less demanding than CFD, but it has the limitations of using a steady state boundary-layer model and a heuristic vorticity decay term (based on matching results obtained from model tests).

3.6. *Orcina wake oscillator*

A wake oscillator model couples a wake equation of motion to the cylinder equation of motion, forming a nonlinear system for predicting vortex excitation in the transverse direction. The system is not derived from physics, but models responses that are characteristic of VIV: oscillatory, self-generating and self-limiting. The model used here is the Milan wake oscillator (Falco et al., 1999).

As with the Orcina vortex tracking model, the structural code *OrcaFlex* is used to compute the response of the riser under the action of flow-induced forces, computed in the time domain on parallel planes.

3.7. *VIVA (MIT)*

VIVA computes transverse responses only, using empirically based rules for vortex excitation (Triantafyllou, 2003). Regions of lock-in are located and are used to identify which of the possible excited modes is most likely to occur. Amplitudes of motion are computed from a database of values for the component of the lift coefficient that may be in phase, or in anti-phase, with the velocity.

VIVA makes two predictions, one for single (complex) modal response and the other assuming that all modes are participating. Although the response shown in this paper is the multi-mode response, the single-frequency response is generally more conservative by an average factor of 1.30.

3.8. *VIVANA (NTNU)*

These computations used the standard released version of VIVANA (Larsen et al., 2000), with the same basic finite element model and options for the hydrodynamic model. This release of VIVANA can calculate cross-flow vibrations only. For present purposes the mean in-line deflection was calculated by applying an amplification factor [given by Vandiver (1983)] to the drag coefficient, to model the effect on the drag of transverse vibrations. Also, VIVANA does not use mode superposition for dynamic analysis and the solution appears at a discrete frequency.

3.9. *VICoMo (NTNU)*

VICoMo uses data from section model tests (Gopalkrishnan, 1993; Wu, 1989) on forced harmonic motions of a cylinder in a plane normal to a steady, uniform current. The conditions were varied systematically to build up a database of force coefficients, as functions of reduced velocity, amplitude and Reynolds number. In VICoMo these coefficients are applied with a strip theory method, in which interactions between flow at neighbouring sections of the riser are neglected.

A finite element approach leads to an eigenvalue problem in which the complex eigenvalue consists of the frequency and the damping of the motion. See Moe et al. (2001) and Moe and Wu (1990) for more details.

3.10. SHEAR7 (MIT)

SHEAR7 is a frequency-domain mode-superposition program. For each mode, zones of excitation are identified by locating regions of the riser where the reduced velocity is within a certain range of the ideal lock-in condition. Elsewhere, the riser is considered to be a source of hydrodynamic damping. Using models for lift and damping forces that depend on the local amplitude and reduced velocity, SHEAR7 iteratively computes an equilibrium condition for each frequency, and combines them to obtain a total response at each point (Vandiver, 1999; Lyons et al., 2003). The results presented here were obtained with SHEAR7 version 4.3e.

3.2. ABAVIV (Technip)

ABAVIV is a time domain code that accounts for structural nonlinearities. The code uses the computer code ABAQUS as the core program, and a VIV methodology based on published models (Finn et al., 1999). Based on the Reynolds number, a Strouhal number of 0.17 was used throughout this analysis. An added mass coefficient of 1.0 was

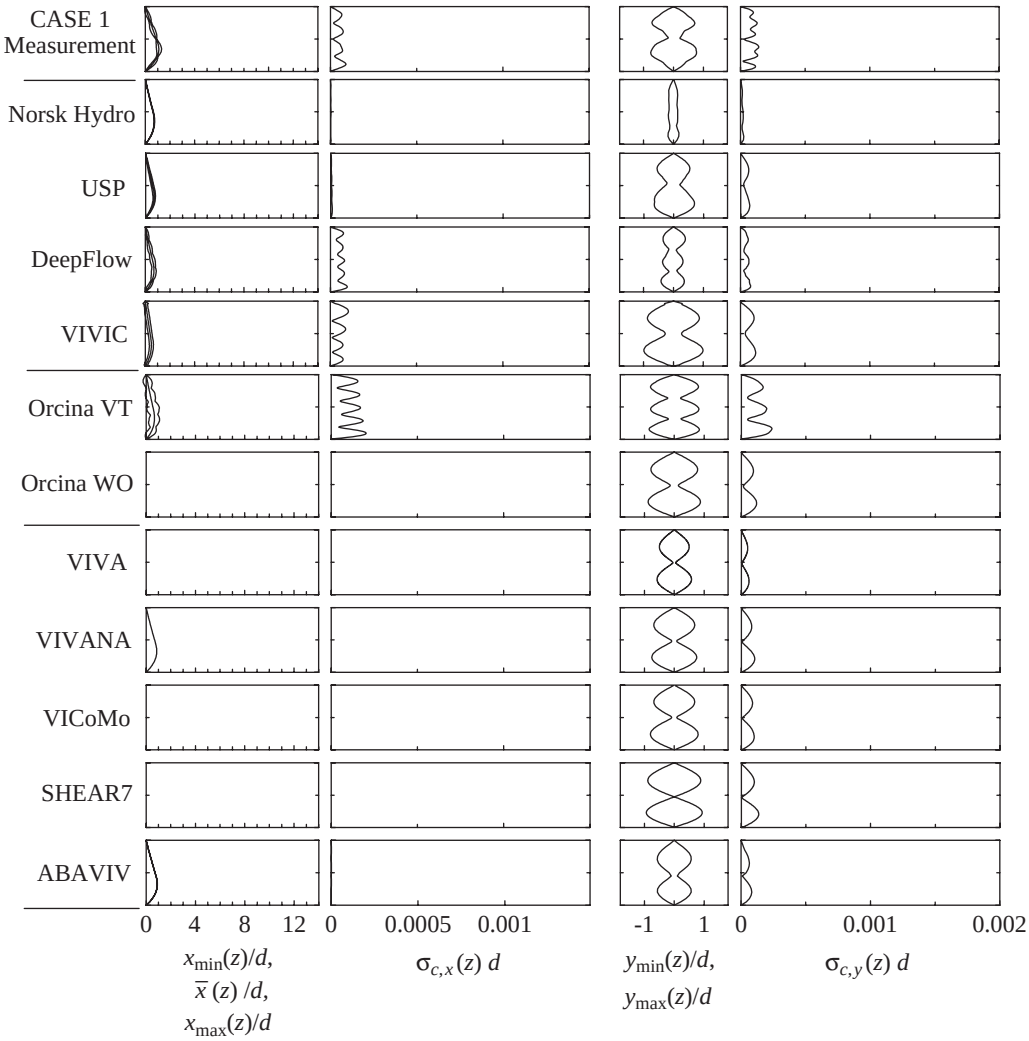

Fig. 2. Envelopes of in-line and cross-flow displacements and curvatures: case 1. The first column of plots shows mean in-line displacements, and (where available) the envelopes of displacements about the mean. The third column shows envelopes of cross-flow displacements. Envelopes of the standard deviation (over time) of in-line and cross-flow curvatures are plotted in the second and fourth columns, respectively.

assumed, neglecting its dependence on the reduced velocity. In addition, a drag coefficient base value of 0.7 was used in the simulation with amplification from VIV. Currently there is no explicit in-line VIV model in ABAVIV, and the in-line response indicated in the results derives from the Morison force with an in-line component from the relative velocity.

4. Results

Measured displacements and curvatures do not always exhibit the well-behaved periodic oscillations that are assumed or are evident in most computed results. This means that extremes in displacements and curvatures measured over long periods are not necessarily directly comparable to peak excursions in the corresponding time series obtained from numerical models. In the laboratory, even very small disturbances can sometimes give rise to significant modulations in the weights of individual modal components, or even a complete redistribution of the response among adjacent modes. For this reason, Chaplin et al. (2005) found that in order to obtain well-behaved measures of response it was often necessary to apply a window to time series of displacements and curvatures, isolating periods of almost steady state motion. The same conditioning was applied to the measured data shown here. Indeed, any comparisons between computed responses and measurements not processed in this way should be approached with some caution.

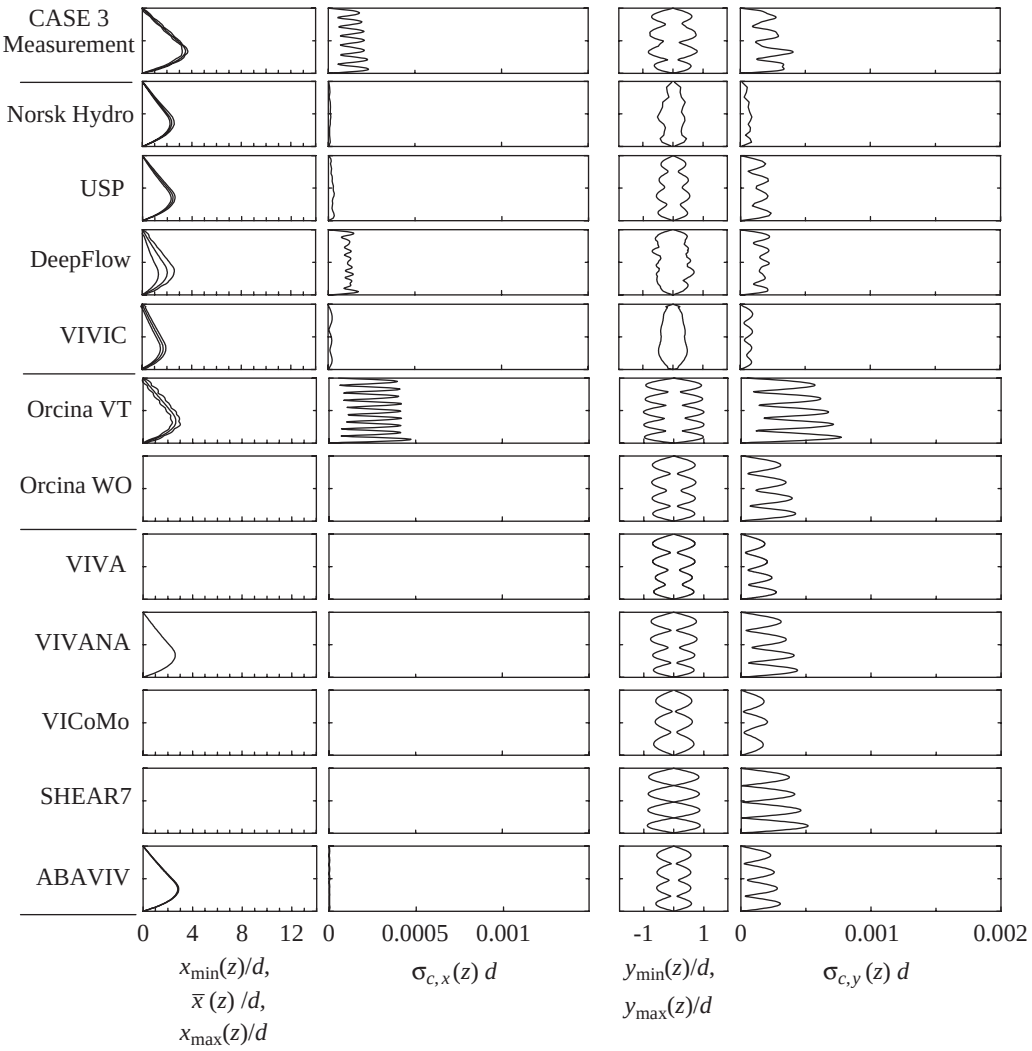

Fig. 3. Envelopes of in-line and cross-flow displacements and curvatures: case 3.

Results are presented first for cases 1–9, a series of tests at carriage speeds between 0.16 and 0.95 m/s, all with the same still water tension. Not all cases were computed with all codes.

4.1. Cases 1–9

4.1.1. Envelopes of in-line displacements and curvatures

The envelopes of measured displacements and curvatures used here as a basis for comparison refer in each case to a period of 10 vortex-shedding cycles from a window in which the riser's motion maintained a steady state, starting at least 20 s after the beginning of the run. For test cases 1, 3, 6 and 9, Figs. 2–5, respectively, show results from the measurements (in the top row) and then row by row from each of the numerical models in the sequence followed above, beginning with the four CFD-based codes. In each case the results are plotted over the length of the riser, from the bottom to the top. The plots in the left-hand column show the mean in-line displacements and the envelopes of in-line displacements around the means. Envelopes of cross-flow displacements are in the third column. The second and fourth columns show envelopes of root-mean-square in-line and cross-flow curvatures.

All of the predictions underestimate the mean in-line displacements of the riser. In the four CFD-based codes, it seems likely that this may be linked to the fact that they under-estimated the amplitude of cross-flow motion, and therefore the associated amplification of drag. However, this does not apply to the Orcina vortex tracking model, in which forces on the riser are similarly computed (albeit less rigorously) from the dynamics of the flow field. In this model, cross-flow responses were considerably larger than the measurements.

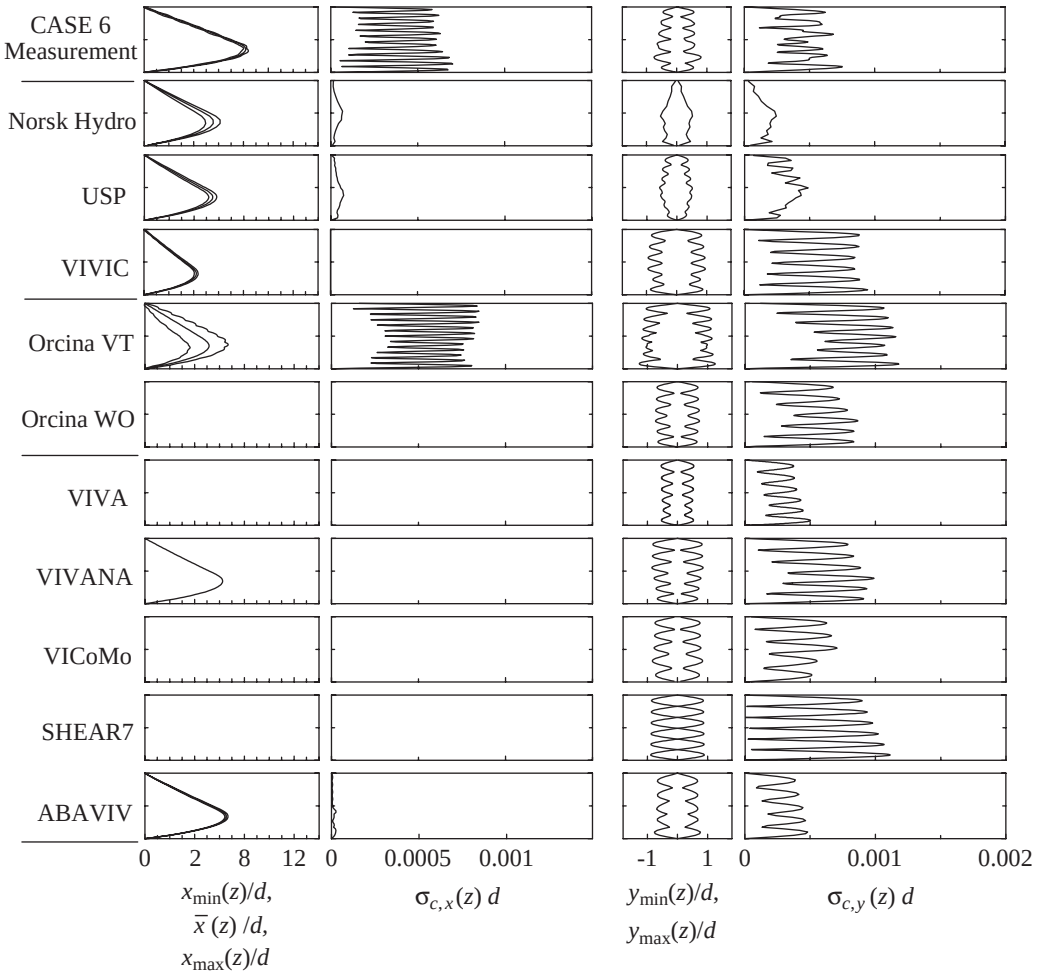

Fig. 4. Envelopes of in-line and cross-flow displacements and curvatures: case 6.

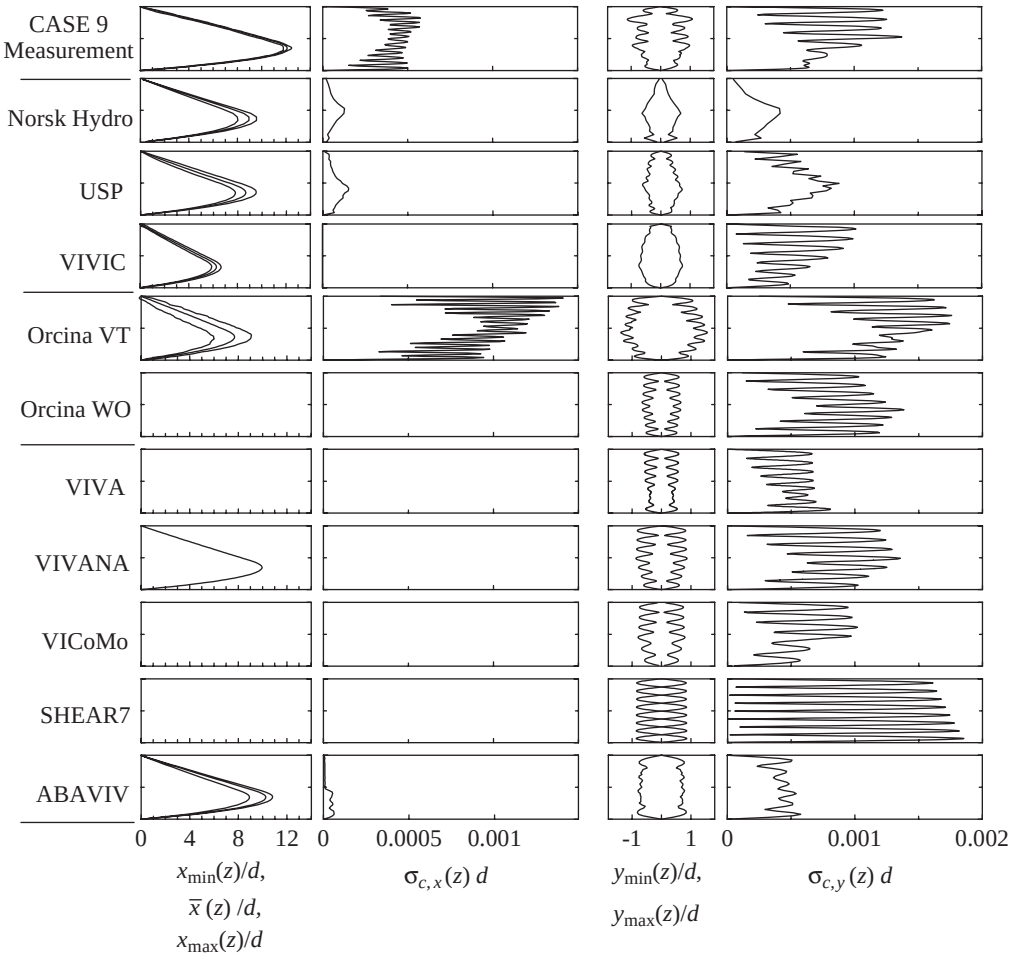

Fig. 5. Envelopes of in-line and cross-flow displacements and curvatures: case 9.

Among the codes represented in the lowest six sets of the plots in each of Figs. 2–5, only VIVANA and ABAVIV predict in-line displacements. In both of these, the mean offsets were obtained by applying Vandiver's (1983) empirical formula for the drag amplification, and the results are in close agreement with each other. The cross-flow displacements predicted by these codes were closer to the measurements than those of the CFD-based codes. Moreover, the measured drag enhancement was found to be in reasonable agreement with Vandiver's formula (Chaplin et al., 2005). It seems likely therefore that the discrepancies between measured and predicted mean in-line displacements in VIVANA and ABAVIV (and perhaps also in other codes) may have more to do with the structural modelling than the computation of the flow-induced forces. The presence of springs at the top of the riser added considerably to the complexity of computing large amplitude displacements, and the springs were not accurately represented in all of the numerical models. It can easily be shown that the extra length provided by the time-average extension of the top springs has a potentially significant effect on mean in-line displacements. In the case of the results from VIVANA and ABAVIV, it would be responsible for increases in the maximum mean in-line displacements of about 50%, which would then exceed the corresponding measured displacements by at least 10%.

None of the empirically based codes predicted in-line vibrations due to vortex shedding. The in-line displacements shown for ABAVIV were computed simply from the relative-velocity Morison equation. Among the other numerical models there are considerable variations, almost all of them showing larger amplitudes of in-line vibrations than in the measurements—notwithstanding the potential effect of shortcomings in nonlinear structural modelling which would tend to lead to under-estimates of vibration amplitudes.

Predicted in-line curvatures reveal a wide range of results, generally in poor agreement with the measurements. This is of interest, because in practice the fatigue damage associated with in-line vibrations may exceed that due to cross-flow vibrations.

4.1.2. Envelopes of cross-flow displacements and curvatures

The effect of the extension of the top springs is much less important in connection with cross-flow vibrations, which were not large enough to invoke any significant nonlinear behaviour of the combined structure. In most cases the measured cross-flow displacements revealed a clear pattern of standing waves. Exceptions were those in which the motion was close to switching from one mode (or combination of modes) to another. In these conditions a standing wave pattern would appear, particularly (as here in case 9, Fig. 5) in the lower part of the riser which was exposed to the current.

Generally the CFD-based predictions of peak cross-flow displacements and curvatures (shown in the third and fourth columns of plots in Figs. 2–5) are considerably smaller than the measurements. This is consistent with the conclusion that two-dimensional CFD codes are incapable of adequately predicting the response envelope even for the case of vortex-induced vibrations of a stiff cylinder on springs (Blackburn et al., 2000). There is more variation among the results from other numerical models, particularly in the curvatures which are strongly affected by the empirical selection of the dominant mode.

4.1.3. Peak displacements and curvatures

Figs. 6–8 compare measurements and predictions of maximum displacements and root-mean-square curvatures for all of cases 1–9. Some of the measurements appear rather scattered, but when the data from all test-series are plotted together as a function of reduced velocity, they form well-ordered families separated by jumps at the transition between one pattern of dominant modes and the next (Chaplin et al., 2005). The numerical results plotted in Figs. 6–8 broadly follow the behaviour seen in Figs. 2–5; maximum mean in-line displacements are underpredicted by all, and there is considerable scatter among predictions of in-line vibration amplitudes. In the cross-flow direction, CFD-based codes generally underpredict peak displacements, the Orcina vortex tracking model is very conservative, and most of the other results are scattered around the measurements. Predictions of in-line curvatures are sparse, and are not in good agreement with the measurements.

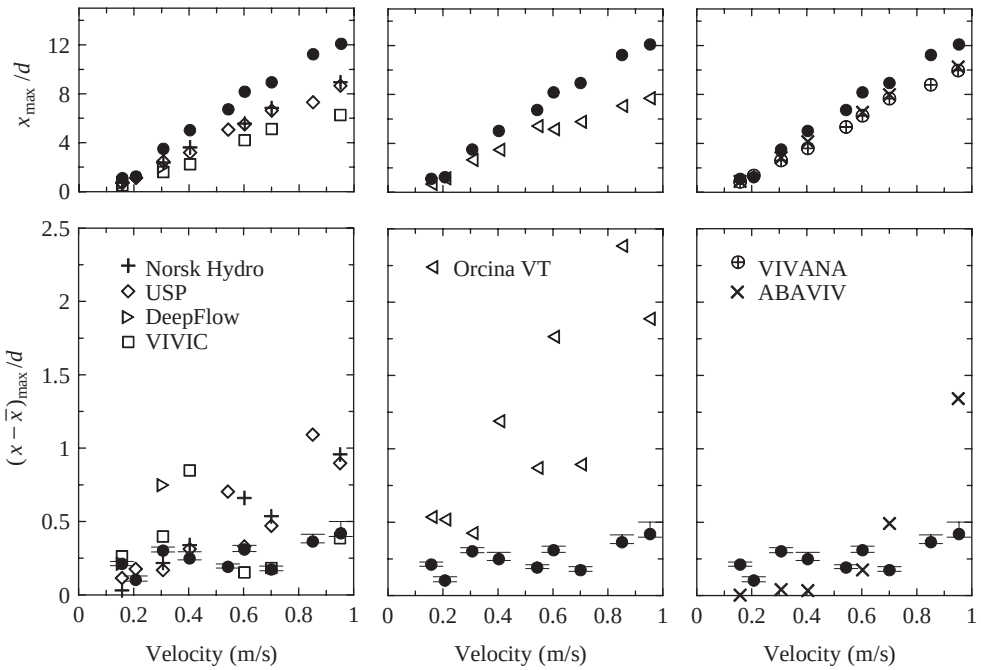

Fig. 6. Maximum mean in-line displacements (top row) and maximum in-line departures from the mean (bottom row): cases 1–9. The measurements are shown as solid circles. In the lower plots the error bars extend one standard deviation in each direction.

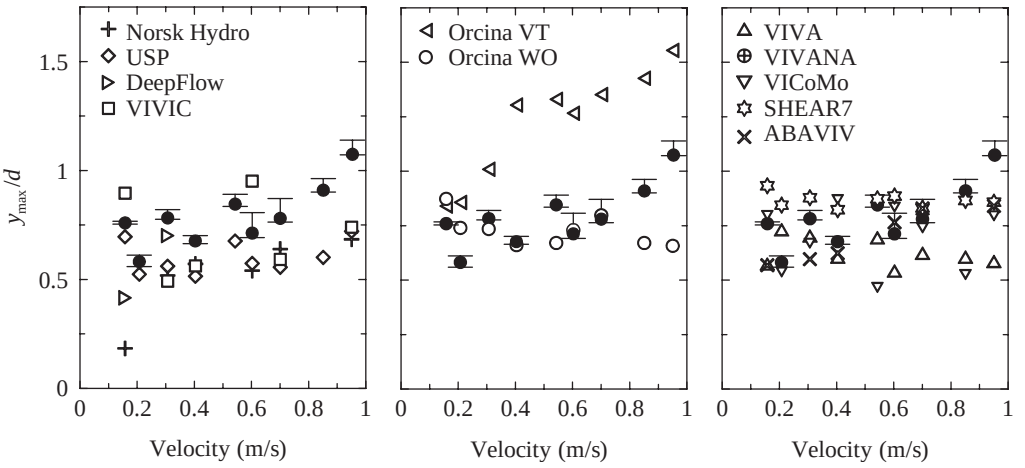

Fig. 7. Peak cross-flow displacements: cases 1–9. The 95-percentile level of measured peak displacements are shown as solid circles. Error bars extend up to the highest peak displacements observed during each test, and down to the 90-percentile level.

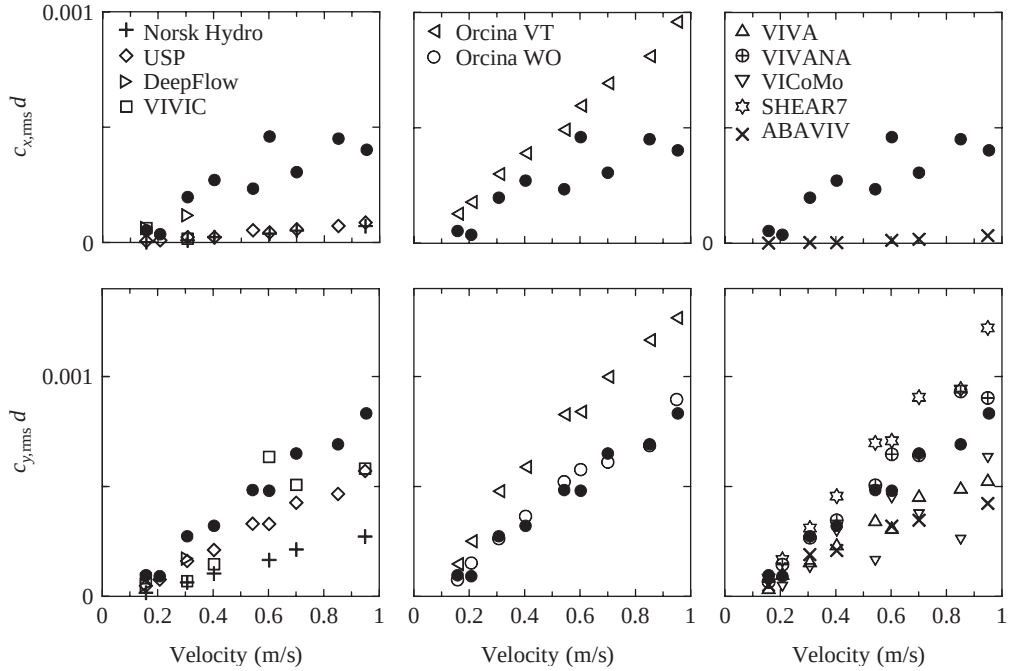

Fig. 8. Curvatures in the in-line (above) and cross-flow (below) directions in cases 1–9. The data shown are the root-mean-square values (over the length of the riser) of the standard deviations (over time). Measurements are shown as solid circles.

4.1.4. Frequencies and mode numbers

Those numerical models that work in the frequency domain identify one frequency, or a small number of frequencies, at which the computed cross-flow response occurs. Generally, each one is associated with a particular mode shape. In time-domain models, on the other hand, the dominant frequencies and mode numbers must be obtained by post-processing the computed time histories of displacements, and this sometimes leads to a distribution of spatial and temporal frequency components that are much less well-defined. Of course, to identify frequencies and modal composition the same procedure has to be applied to the measurements, but in this case it was possible to work with longer time series of steady state oscillations, and the dominant frequency components of the response could be clearly identified without much difficulty.

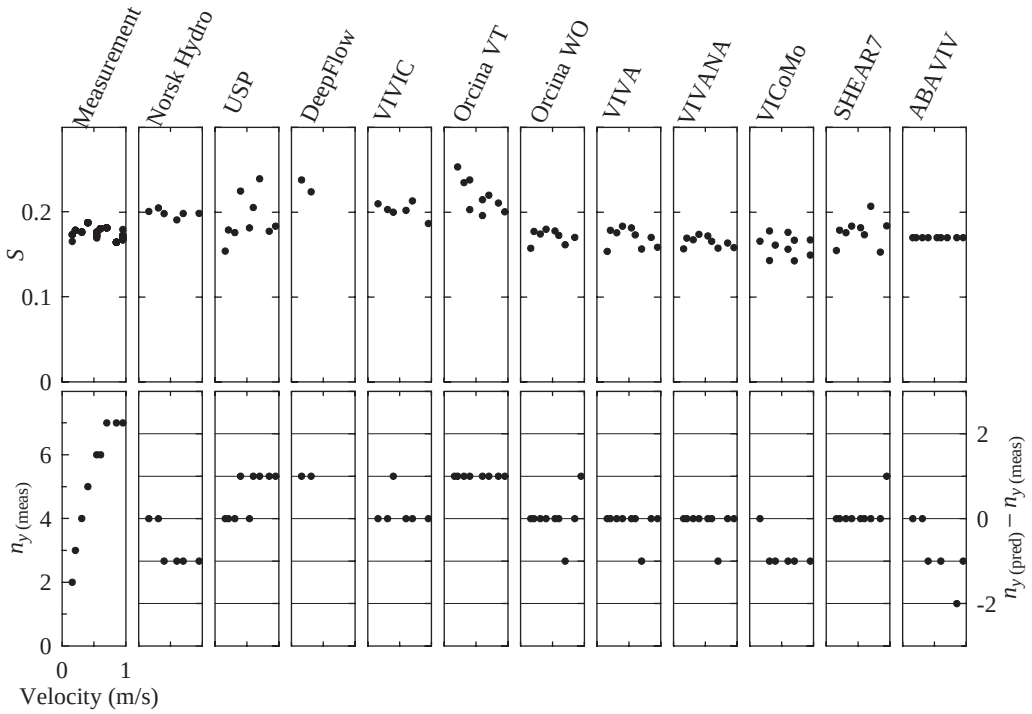

Fig. 9. In the upper row of plots the dominant frequency in the cross-flow vibrations (expressed as a Strouhal number) is shown as a function of the velocity. The first plot of the lower row shows the dominant mode number of the measured cross flow vibration. The remaining plots in the lower row show the predicted dominant mode number relative that observed in the measurements. Cases 1–9.

The top row of plots in Fig. 9 shows the single dominant temporal frequency (in the form of a Strouhal number, and associated where appropriate with the largest single modal component with a frequency in the region of a Strouhal number of 0.2) from the measurements and from each numerical model, plotted against the carriage speed. With the exception of ABAVIV (in which the oscillation frequency is fixed at a Strouhal number of 0.17), most frequencies from the empirically based models VIVA, VIVANA, VICoMo and SHEAR7 (and the Orcina Wake Oscillator model) follow the same behaviour, and as might be expected they are all close to the measured frequencies (also about 0.17).

There is much more variation among the time-domain models, and as mentioned above this may be partly associated with computational issues. Many of these models reported several closely spaced frequencies in the region of $S = 0.2$, of which only the one associated with the largest modal amplitude is shown here. There is a clear pattern to be seen in the frequencies of measured cross-flow responses, and [as discussed by Chaplin et al. (2005)] this can be associated with lock-in with an ascending sequence of modes. This behaviour was not evident in results from any of the CFD-based codes. (A series of test cases at more closely spaced velocities might have been more revealing in this respect.)

The first plot of the lower row in Fig. 9 shows the dominant mode number $n_{y(\mathrm{meas})}$ of the measured cross-flow response. For each test case the remaining plots in the row show the difference between the modal numbers of predicted and measured cross-flow responses $n_{y(\mathrm{pred})} - n_{y(\mathrm{meas})}$. In almost all cases the difference is no greater than 1.

4.2. Cases 10–15

Cases 10–15 comprise two series of tests with top tensions that were higher than those of cases 1–9. Predictions were carried out with only 6 of the numerical models, and the results for maximum mean in-line displacements, maximum cross-flow displacements, and maximum root-mean-square cross-flow curvatures are collected in Fig. 10. In these cases, the initial tension in the riser was higher than in cases 1–9, and so at a given speed the in-line displacement was considerably smaller.

In comparison with the measured results, shown as solid bars in Fig. 10, the predictions follow trends similar to those discussed above. The maximum in-line displacement was underestimated in every case, and there was a wide variation in predicted peak curvatures. On the whole, cross-flow displacements obtained from the empirically based codes were

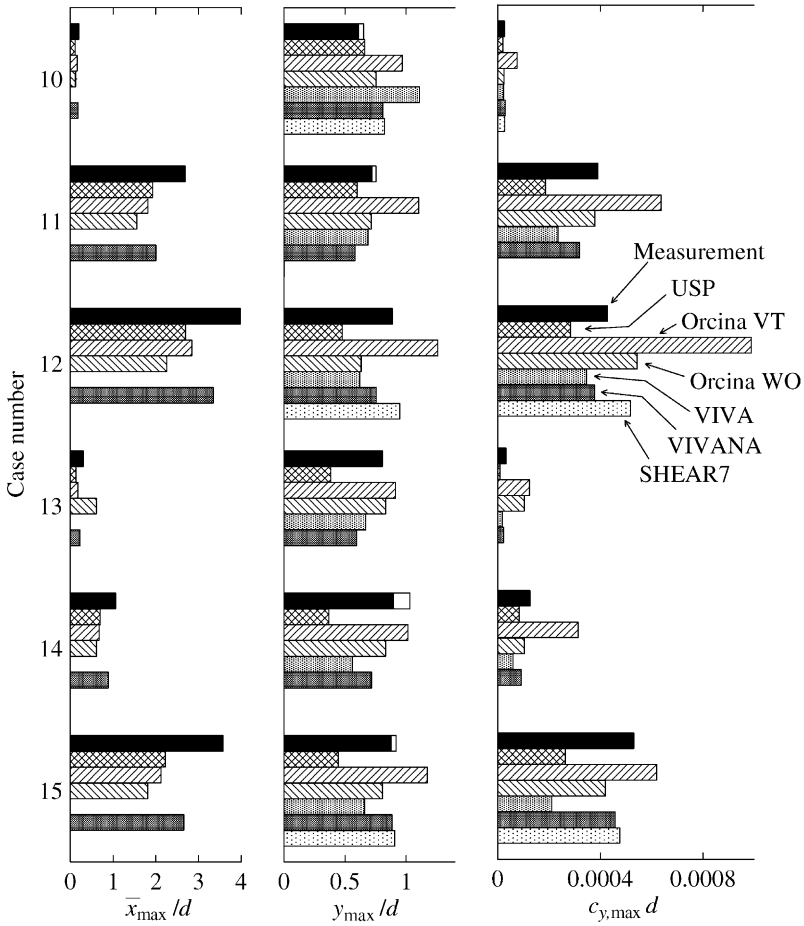

Fig. 10. Measured and predicted results for cases 10–15. Maximum cross-flow displacements are shown by solid bars up to the 95-percentile level. The open bars extend to the peak displacement observed over the whole of each test run.

closer to the measurements than the predictions of the USP code, the only CFD-based model for which results are available.

4.3. Overall ratios between predictions and measurements

As an overall indication of the proximity of each set of numerical predictions to the measurements, Fig. 11 shows ratios $\langle \bar{x}_{\max}/d \rangle$ etc. with the notation

$$\langle \bullet \rangle = \frac{1}{N} \sum_{n=1}^{N} \frac{[\bullet]_{n,\text{predicted}}}{[\bullet]_{n,\text{measured}}},$$

where N is the number of cases computed with a particular model.

As mentioned above, the low predictions of mean in-line displacements (Fig. 11(a)) may be associated with some uncertainty over the modelling of the effect of the top springs, but this is not likely to affect other results to the same extent. Among the other parameters, predictions of in-line curvatures (though available from only six of the models) show the widest spread around the measurements. It should be noted that those from DeepFlow and VIVIC were computed only for 2 cases, at velocities less than 0.4 m/s.

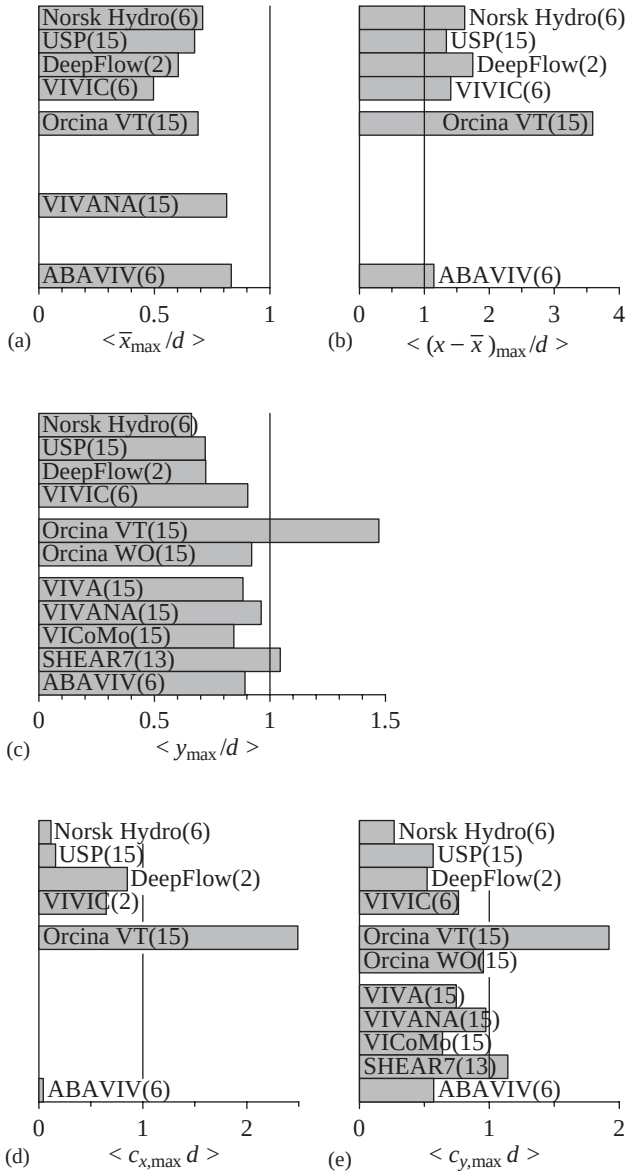

Fig. 11. Overall average ratios of predictions to measurements; (a) maximum mean in-line displacement, (b) maximum in-line displacements from the mean, (c) maximum cross-flow displacements, (d) and (e) maximum in-line and cross-flow standard deviations of curvatures. Numbers in parentheses denote the total number of predictions computed with each numerical model.

5. Conclusions

Blind predictions of laboratory measurements of the vortex-induced vibrations of a model riser in a stepped current [described in detail by Chaplin et al. (2005)], have been carried out with 11 different numerical models. These included CFD-based codes, in which the three-dimensional nature of the flow around the riser is modelled by two-dimensional calculations on a large number of parallel planes communicating only through the structural response, and empirical models based on an empirical understanding of vortex-induced vibrations in two-dimensional conditions.

On average, over all cases computed by each model, predictions of cross-flow displacements from the empirically based codes (VIVA, VIVANA, VICoMo, SHEAR7 and ABAVIV) and the Orcina Wake Oscillator code were all between 85% and 105% of the corresponding measurements. (Displacements and curvatures from VIVA are for the

multi-mode response, rather than the more conservative single frequency response.) Results of the CFD-based codes (Norsk Hydro, USP, DeepFlow and VIVIC) were characterized by smaller cross-flow displacements, with ratios of predictions to measurements (mostly over a reduced set of test cases) in the range 65–90%. Predictions of vortex-induced in-line dynamic displacements were provided only by the CFD-based codes, and average ratios were between 135% and 175%.

For individual test cases, errors were sometimes much larger. There was also considerably more variation among predicted curvatures. In-line curvatures computed with the two CFD-based codes that reported results over the whole range of test cases were on average less than 20% of the corresponding measurements. For cross-flow curvatures, average ratios for 10 of the 11 codes were between 25% and 115%.

The Orcina vortex-tracking model alone was very conservative, overestimating dynamic in-line displacements and both in-line and cross-flow curvatures by 100% or more, and cross-flow displacements by 50%. With this exception, it can be concluded that the empirically based models were more successful at predicting cross-flow displacements than those based on CFD. The same applies to cross-flow curvatures (though these results were more scattered). But in-line vortex-induced curvatures, which in practice may cause as much damage as cross-flow curvatures, could not be computed by any of the empirically based codes, and in general those based on CFD codes were in very poor agreement with the measurements.

It is interesting to note that these predictions reveal a much better degree of consensus than those of an earlier exercise conducted by Larsen and Halse (1995). In that case (in the absence of any measurements), the results of seven numerical models were compared with each other. A measure of progress over the last 10 years is provided by the fact that in many respects the predictions of a wide range of models are now seen to be in reasonable agreement.

Acknowledgements

The compilation of data presented above was carried out as part of a project on vortex-induced vibrations of deep water risers, supported by the EPSRC. We are also indebted to BP for access to commercial software.

References

Blackburn, H.M., Govardhan, R.N., Williamson, C.H.K., 2000. A complementary numerical and physical investigation of vortex-induced vibration. Journal of Fluids and Structures 15, 481–488.

Chaplin, J.R., Bearman, P.W., Fontaine, E., Herfjord, M., Isherwood, M., Larsen, C.M., Meneghini, J.R., Moe, G., Triantafyllou, M.S., 2004. Blind predictions of laboratory measurements of vortex-induced vibrations of a tension riser. In: de Langre, E., Axisa, F. (Eds.), Proceedings of the Eighth International conference on Flow-Induced Vibration, Paris, France, vol. 2, pp. 285–290.

Chaplin, J.R., Bearman, P.W., Huera Huarte, F.J., Pattenden, R.J., 2005. Laboratory measurements of vortex-induced vibrations of a vertical tension riser in a stepped current. Journal of Fluids and Structures 21, 3–24.

DeepLines, 2002. Multi-Lines Floating Systems analysis, Theory Manual, version 3r1, Institut Français du Pétrole, Principia Recherche et Développement.

Eberg, E., Hellan, Ø., Amdahl, J., 1993. Non-linear reassessment of jacket structure under extreme storm cyclic loading. In: Proceedings of the 12th International conference on Offshore Mechanics and Arctic Engineering, ASME, New York vol. 1, pp. 517–523.

Etienne, S., 1999. Contribution a la modélisation de l'écoulement de fluide visqueux autour de faisceaux de cylindres circulaires. Ph.D. Thesis, Université de la Méditerranée, Aix-Marseille II, France.

Falco, M., Fossati, F., Resta, F., 1999. On the vortex induced vibration of submarine cables: design optimization of wrapped cables for controlling vibrations. In: Proceedings of the Third International Symposium on Cable Dynamics, Trondheim, Norway.

Ferrari, J.A., 1998. Hydrodynamic loading and response of offshore risers. Ph.D. Thesis, University of London, UK.

Finn, L., Lambrakos, K., Maher, J., 1999. Time domain prediction of riser VIV. In: Proceedings of the Fourth International Conference on Advances in Riser Technologies, Aberdeen, Scotland.

Gopalkrishnan, R., 1993. Vortex-Induced forces on oscillating bluff cylinders. Ph.D. Thesis, Department of Ocean Engineering, Massachusetts Institute of Technology, Cambridge, MA, USA.

Herfjord, K., 1996. A study of two-dimensional separated flow by a combination of the Finite Element method and Navier-Stokes equations. Ph.D. Thesis, Department of Marine Hydrodynamics, Norwegian University of Science and Technology, Trondheim, Norway.

Herfjord, K., Drange, S.O., Kvamsdal, T., 1999. Assessment of vortex-induced vibrations on deepwater risers by considering fluid-structure interaction. ASME Journal of Offshore Mechanics and Arctic Engineering 121, 207–212.

Herfjord, K., Holmås, T., Randa, K., 1998. A parallel approach for numerical solution of vortex induced vibrations of very long risers. In: Proceedings of the Fourth World Congress on Computational Mechanics, Buenos Aires, Argentina.

Larsen, C.M., Halse, K.H., 1995. Comparison of models of vortex-induced vibrations of slender marine structures. In: Bearman, P.W. (Ed.), Flow-Induced Vibration. Balkema, Rotterdam, pp. 467–482.

Larsen, C.M., et al., 2000. VIVANA—Theory manual. MARINTEK 513102.01, Trondheim, Norway.

Lyons, G.J., Vandiver, J.K., Larsen, C.M., Ashcombe, G.T., 2003. Vortex induced vibrations measured in service in the Foinaven dynamic umbilical, and lessons from prediction. Journal of Fluids and Structures 17, 1079–1094.

Moe, G., Arntsen, Ø., Hoen, C., 2001. VIV analysis of risers by complex modes. In: Proceedings of the 11th International Offshore and Polar Engineering Conference, vol. 3, pp. 426–430.

Moe, G., Wu, Z.-J., 1990. The lift force on a cylinder vibrating in a current. Journal of Offshore Mechanics and Arctic Engineering 112, 297–303.

Patel, M.H., Witz, J.A., 1991. Compliant Offshore Structures. Butterworth, UK.

Sarpkaya, T., Shoaff, R.L., 1979. Inviscid model of two-dimensional vortex shedding by a circular cylinder. AIAA Journal 17, 1193–1200.

Triantafyllou, M.S., 2003. VIVA Extended User's Manual. Massachusetts Institute of Technology, Department of Ocean Engineering, Cambridge, MA, USA.

Vandiver, J.K., 1983. Drag coefficients of long flexible risers. Offshore Technology Conference OTC Number 4490.

Vandiver, J.K., 1999. User Guide for SHEAR7. Massachusetts Institute of Technology, Department of Ocean Engineering, Cambridge, MA, USA.

Willden, R.H.J., 2003. Numerical prediction of the vortex-induced vibrations of marine riser pipes. Ph.D. Thesis, University of London, UK.

Willden, R.H.J., Graham, J.M.R., 2004. Multi-modal vortex-induced vibrations of a vertical riser pipe subject to a uniform current profile. European Journal of Mechanics B/Fluids 23, 209–218.

Wu, Z.-J., 1989. Current induced vibrations of a flexible cylinder. Dr.ing Thesis, Department of Civil Engineering, Norwegian University of Science and Technology, Trondheim, Norway.

Yamamoto, C.T., Fregonesi, R.A., Meneghini, J.R., Saltara, F., Ferrari, J.A., 2004. Numerical simulations of vortex-induced vibration of flexible cylinders. Journal of Fluids and Structures 19, 467–489.